



Indian Academy of Sciences, Bengaluru
Indian National Science Academy, New Delhi
The National Academy of Sciences India, Prayagraj
SUMMER RESEARCH FELLOWSHIPS — 2025

Format for the final Report^{*, ^}

Name of the candidate : PALLU KUMAR

Application Registration no. : ENGS3179

Date of joining : 16/05/2025

Date of completion : 12/07/2025

Total no. of days worked : 58

Name of the guide : Prof Prabhu R Nott

Guide's institution : Indian Institute of Science (IISc), Bengaluru, Karnataka

Project title : Modelling of Slow Granular Flow

Address with pin code to which the certificate could be sent:

Aryabhata Hostel, IIT(BHU), Varanasi, UP-221005

E-mail ID: pallu.kumar.cd.che23@itbhu.ac.in

Phone No: 8221031394

TA Form attached with final report : YES Yes NO

If, NO, Please specify reason

Pallu Kumar

Signature of the candidate

Date: 17/07/2025

Signature of the guide

Date: 17-07-2025

IMPORTANT NOTES:

* This format should be the first page of the report and should be stapled with the main report. The final report could be anywhere between 20 and 25 pages including tables, figures etc.

^ The final report must reach the Academy office within 10 days of completion. If delayed fellowship amount will not be disbursed.

(For office use only; do not fill/tear)

Candidate's name:	Fellowship amount:
Student: Teacher:	Deduction:
Guide's name:	TA fare:
KVPY Fellow: INSPIRE Fellow:	Amount to be paid:
PFMS Unique Code:	A/c holder's name:
Others	

Summer Research Fellowship Program 2025

Final Report

Submitted by

Pallu Kumar

IIT (BHU), Varanasi

Department of Chemical Engineering

Application No: ENGS3179

Under the guidance of

Prof. Prabhu R Nott

Department of Chemical Engineering

Indian Institute of Science, Bengaluru

Contents

1	Introduction	2
1.1	Granular Materials and Flow Regimes	2
1.2	Modelling of Intermediate Regime	2
1.3	Non-local Continuum Model for Slow Granular Flow	3
2	Plane Shear: Analytical Derivation	3
2.1	Problem Description	3
2.2	Derivation	4
2.2.1	Governing Equations	4
2.2.2	Assumptions	5
2.2.3	Simplifying Equations Based on Assumptions	5
3	Numerical Solution	9
3.1	Methodology: Finite Difference Method (FDM)	9
3.1.1	Basic Idea of the Finite Difference Method	9
3.1.2	Method of Undetermined Coefficients for Finite Difference Formulas . .	10
3.2	Model Predictions for simple shear	11
3.2.1	Governing Equations	11
3.2.2	Boundary Conditions	11
3.2.3	Numerical Implementation	11
3.2.4	Results and Discussion	12
3.3	Model Predictions for Couette flow	14
3.3.1	Governing Equations	14
3.3.2	Boundary Conditions	15
4	MATLAB Implementation	17
4.1	Finite Difference Coefficient Determination	17
5	Conclusion	20
6	Acknowledgement	21
	References	22

1. Introduction

1.1. Granular Materials and Flow Regimes

Granular materials are collections of rigid, macroscopic particles typically larger than $100\ \mu\text{m}$ that interact primarily through contact forces such as friction and collision, and behave collectively as solids, liquids, or gases depending on the external conditions. Granular materials, such as sand, grains, and catalyst particles, are found in a wide range of natural and industrial environments. Yet, their flow behavior remains challenging to model due to the complexity arising from solid-like and fluid-like interactions. Granular flow refers to the collective motion of densely packed grains driven by external forces, where the momentum transport is governed by a combination of interparticle collisions and enduring contacts.

The dynamic behavior of granular flows is classified into distinct regimes based on the mechanism of momentum transfer. A crucial dimensionless parameter used to characterize the flow regime of granular media is the *inertial number* I , which describes the relative importance of inertia and confining stresses:

$$I = \frac{d \dot{\gamma}}{\sqrt{p/\rho_p}}$$

where d is the characteristic particle diameter, $\dot{\gamma}$ is the local shear rate, p is the pressure, and ρ_p is the particle density.

This number distinguishes between the quasistatic flow regime (low I), the collisional or rapid flow regime (high I), and intermediate regimes where both frictional contact and inertial effects coexist ($10^{-3} < I < 0.1$). Quasistatic or slow regime flow is dominated by frictional forces with a lesser effect of inertia, while rapid flow is characterized by high shear rates and frequent collisions.

1.2. Modelling of Intermediate Regime

The intermediate regime of granular flow, where both enduring frictional contacts and inertial effects contribute significantly to stress transmission, poses a major challenge in continuum modelling due to the coexistence of solid- and fluid-like behavior. Traditional local rheological models fail to capture important features such as shear localization and non-uniform volume fraction profiles. One such local rheology, proposed by GDR MiDi [1], introduces empirical $\mu(I)$ and $\phi(I)$ relations, linking the stress ratio and packing fraction to the inertial number, thereby enabling rate-dependent descriptions of dense flows. This framework was later adopted by Jop *et al.* [2], who formulated the tensorial form of the constitutive relation based on these empirical laws. However, as mentioned above, this local rheology fails to capture many features of granular flows, and the constitutive modelling has consequently shifted towards non-local

continuum models.

1.3. Non-local Continuum Model for Slow Granular Flow

In the regime of dense, slow granular flow, classical local plasticity theories are limited by kinematic indeterminacy and fail to capture essential phenomena such as dilatancy and shear localization. To address these limitations, Dsouza and Nott [3] proposed a non-local constitutive model by extending critical state plasticity into a volume-averaged framework.

The core idea is that plastic deformation and dilation at a point are influenced not only by the local yield condition but also by the stress state in a surrounding mesoscopic volume. This leads to a stress–deformation relationship incorporating spatial gradients of strain rate and density, thereby enabling the model to capture shear-induced dilatancy. The model demonstrated strong agreement with DEM simulations in reproducing velocity and volume fraction profiles in simple shear flows.

The non-local constitutive relations are given by:

$$\boldsymbol{\sigma} = -p\boldsymbol{\delta} + 2\mu\dot{\boldsymbol{\gamma}} \left(p_c \mathbf{D}' - \ell^2 \Pi \nabla^2 \mathbf{D}' \right), \quad (1.1a)$$

$$p_c = \Pi - \ell^2 \frac{d\Pi}{d\phi} \nabla^2 \phi, \quad (1.1b)$$

$$p = p_c \left(1 - \mu_b \frac{\nabla \cdot \mathbf{u}}{\dot{\boldsymbol{\gamma}}} \right) + \ell^2 \Pi \mu_b \frac{\nabla^2 (\nabla \cdot \mathbf{u})}{\dot{\boldsymbol{\gamma}}}. \quad (1.1c)$$

Although originally formulated for slow, quasi-static flows (i.e., negligible inertial number), the model structure naturally invites extension to inertial regimes by allowing the macroscopic friction coefficient μ and the critical state pressure function Π to become functions of the inertial number I , analogous to the $\mu(I)$ – $\phi(I)$ rheology commonly used for dense granular flows.

However, whether such a non-local extension, grounded in critical state theory, can accurately predict the complex stress and volume fraction fields observed in the intermediate regime remains an important open problem. In this work, we aim to explore the applicability of this non-local model in intermediate flow regimes where inertia also plays a significant role.

2. Plane Shear: Analytical Derivation

2.1. Problem Description

The plane shear flow configuration analyzed in this study is inspired by the setup considered in Dsouza and Nott [3], and is illustrated in Figure 1. In this setup, a layer of dense granular material is confined between two parallel, rough walls. The top wall moves at a constant velocity

u_w , while the bottom wall remains stationary. This generates a uniform shear across the layer in the absence of gravity, making it a simplified yet insightful configuration for studying the rheology of dense granular flows.

As shown in Figure 1, the walls are constructed using spheres of diameter d_w arranged in a close-packed square array. Periodic boundary conditions are applied along the x - and z -directions, with unit cell dimensions specified as $L = 60d_p$ and $D = 40d_p$, where d_p is the particle diameter of the granular material.

In the present work, we focus exclusively on the gravity-free case. The absence of gravitational effects allows the system to achieve a steady shear flow that is symmetric about the mid-plane and free from pressure or volume fraction gradients induced by body forces. This setting facilitates analytical treatment and helps isolate the effects of the constitutive model on the velocity profile.

To initiate the analysis, we first consider the case where the volume fraction ϕ is uniform across the shear gap. This assumption simplifies the governing equations provided in Dsouza and Nott [3] and permits an analytical solution to be obtained. The resulting expression for the velocity field is derived in the following subsection.

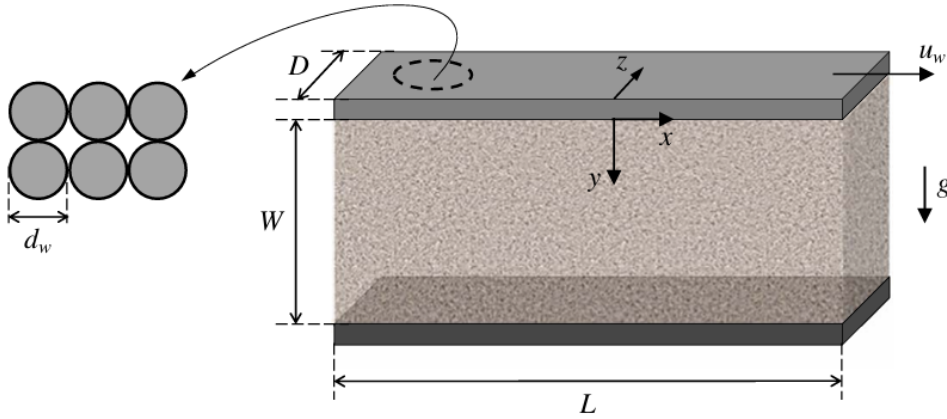


Figure 1: Schematic of plane Couette flow. The top plate is translated with constant velocity u_w and the bottom plate is held stationary. The walls were constructed of spheres of diameter d_w in a close-packed square array. Periodic boundary conditions in the x and z directions were enforced with unit cell dimensions $L = 60d_p$, $D = 40d_p$. (Image taken from Dsouza and Nott [3])

2.2. Derivation

2.2.1. Governing Equations

Mass Balance

$$\frac{\partial \rho}{\partial t} + \frac{\partial(\rho u_x)}{\partial x} + \frac{\partial(\rho u_y)}{\partial y} + \frac{\partial(\rho u_z)}{\partial z} = 0 \quad (2.1)$$

Momentum Balances

x-momentum balance:

$$\rho \left(\frac{\partial u_x}{\partial t} + u_x \frac{\partial u_x}{\partial x} + u_y \frac{\partial u_x}{\partial y} + u_z \frac{\partial u_x}{\partial z} \right) = -\frac{\partial p}{\partial x} + \left[\frac{\partial \tau_{xx}}{\partial x} + \frac{\partial \tau_{yx}}{\partial y} + \frac{\partial \tau_{zx}}{\partial z} \right] + \rho g_x \quad (2.2)$$

y-momentum balance:

$$\rho \left(\frac{\partial u_y}{\partial t} + u_x \frac{\partial u_y}{\partial x} + u_y \frac{\partial u_y}{\partial y} + u_z \frac{\partial u_y}{\partial z} \right) = -\frac{\partial p}{\partial y} + \left[\frac{\partial \tau_{xy}}{\partial x} + \frac{\partial \tau_{yy}}{\partial y} + \frac{\partial \tau_{zy}}{\partial z} \right] + \rho g_y \quad (2.3)$$

z-momentum balance:

$$\rho \left(\frac{\partial u_z}{\partial t} + u_x \frac{\partial u_z}{\partial x} + u_y \frac{\partial u_z}{\partial y} + u_z \frac{\partial u_z}{\partial z} \right) = -\frac{\partial p}{\partial z} + \left[\frac{\partial \tau_{xz}}{\partial x} + \frac{\partial \tau_{yz}}{\partial y} + \frac{\partial \tau_{zz}}{\partial z} \right] + \rho g_z \quad (2.4)$$

2.2.2. Assumptions

1. Steady state
2. Incompressible flow
3. Slow flow regime
4. No gravity
5. Fully developed flow in x-direction ($\frac{\partial}{\partial x} = 0$)
6. No variation in y and z ($\frac{\partial}{\partial x} = 0$, $\frac{\partial}{\partial z} = 0$)
7. 1D flow in x-direction only

2.2.3. Simplifying Equations Based on Assumptions

Mass Balance

$$\frac{\partial}{\partial x}(\rho u_x) = 0 \quad (\text{Trivially Satisfied})$$

x-momentum balance

$$0 = -\frac{\partial p}{\partial x} + \frac{\partial}{\partial y}(\tau_{yx})$$

y-momentum balance

$$0 = -\frac{\partial p}{\partial y} + \frac{\partial}{\partial y}(\tau_{yy})$$

z-momentum balance

$$0 = -\frac{\partial p}{\partial z} + \frac{\partial}{\partial y}(\tau_{yz})$$

Now, incorporating the non-local model given by Dsouza and Nott [3]:

$$\begin{aligned}\sigma &= -p\delta + \frac{2\mu}{\dot{\gamma}} \left(p_c \mathbf{D}' - l^2 \Pi \nabla^2 \mathbf{D}' \right) \\ p_c &= \Pi - l^2 \frac{d\Pi}{d\phi} \nabla^2 \phi \\ p &= p_c \left(1 - \frac{\mu_b \nabla \cdot \mathbf{u}}{\dot{\gamma}} \right) + l^2 \Pi \frac{\mu_b}{\dot{\gamma}} \nabla^2 (\nabla \cdot \mathbf{u})\end{aligned}$$

Deformation Rate Tensor \mathbf{D}

$$\mathbf{D} = \frac{\nabla \mathbf{u} + (\nabla \mathbf{u})^T}{2}$$

$$\mathbf{D} = \begin{bmatrix} \frac{\partial u_x}{\partial x} & \frac{1}{2} \left(\frac{\partial u_x}{\partial y} + \frac{\partial u_y}{\partial x} \right) & \frac{1}{2} \left(\frac{\partial u_x}{\partial z} + \frac{\partial u_z}{\partial x} \right) \\ \frac{1}{2} \left(\frac{\partial u_y}{\partial x} + \frac{\partial u_x}{\partial y} \right) & \frac{\partial u_y}{\partial y} & \frac{1}{2} \left(\frac{\partial u_y}{\partial z} + \frac{\partial u_z}{\partial y} \right) \\ \frac{1}{2} \left(\frac{\partial u_z}{\partial x} + \frac{\partial u_x}{\partial z} \right) & \frac{1}{2} \left(\frac{\partial u_z}{\partial y} + \frac{\partial u_y}{\partial z} \right) & \frac{\partial u_z}{\partial z} \end{bmatrix}$$

$$\mathbf{D}' = \mathbf{D} \quad (\nabla \cdot \mathbf{u} = 0, \text{ from incompressible assumption})$$

Now, simplifying \mathbf{D}' based on our problem:

$$\mathbf{D}' = \begin{bmatrix} 0 & \frac{1}{2} \frac{\partial u_x}{\partial y} & 0 \\ \frac{1}{2} \frac{\partial u_x}{\partial y} & 0 & 0 \\ 0 & 0 & 0 \end{bmatrix}$$

Finding Expression for Shear Rate $\dot{\gamma}$

$$\begin{aligned}\dot{\gamma} &= (2\mathbf{D}' : \mathbf{D}')^{1/2} \\ \dot{\gamma} &= \left[2 \left(\frac{1}{2} \frac{\partial u_x}{\partial y} \right)^2 \right]^{1/2} \\ \dot{\gamma} &= \left| \frac{\partial u_x}{\partial y} \right|\end{aligned}$$

Non-local Model Stress Components

$$\begin{aligned}
 \tau_{yx} &= \frac{2\mu}{\dot{\gamma}} \left(p_c D'_{yx} - l^2 \Pi \nabla^2 D'_{yx} \right) \\
 &= \frac{2\mu}{\dot{\gamma}} \left(p_c \frac{1}{2} \frac{\partial u_x}{\partial y} - l^2 \Pi \frac{1}{2} \frac{\partial^3 u_x}{\partial y^3} \right) \\
 &= \frac{\mu}{\dot{\gamma}} \left(p_c \frac{\partial u_x}{\partial y} - l^2 \Pi \frac{\partial^3 u_x}{\partial y^3} \right)
 \end{aligned}$$

Similarly,

$$\tau_{xy} = \frac{\mu}{\dot{\gamma}} \left(p_c \frac{\partial u_x}{\partial y} - l^2 \Pi \frac{\partial^3 u_x}{\partial y^3} \right)$$

where $u_x = f(y)$ only.

$$\begin{aligned}
 \tau_{yy} &= \frac{2\mu}{\dot{\gamma}} \left(p_c D'_{yy} - l^2 \Pi \nabla^2 D'_{yy} \right) \\
 \tau_{yy} &= 0 \\
 \tau_{yz} &= \frac{2\mu}{\dot{\gamma}} \left(p_c D'_{yz} - l^2 \Pi \nabla^2 D'_{yz} \right) \\
 \tau_{yz} &= 0
 \end{aligned}$$

x-momentum:

$$0 = \frac{d}{dy} \left(\frac{\mu p_c}{\dot{\gamma}} \frac{du_x}{dy} - \frac{\ell^2 \mu \Pi}{\dot{\gamma}} \frac{d^3 u_x}{dy^3} \right)$$

y-momentum:

$$\begin{aligned}
 \frac{dp}{dy} &= 0 \\
 \Rightarrow p &= \text{constant}
 \end{aligned}$$

When ϕ does not vary with y , $p_c = \Pi$ from the constitutive relation. Also, $p = p_c$ (since $\nabla \cdot \mathbf{u} = 0$).

z-momentum:

$$\frac{dp}{dz} = 0$$

Finally, we have:

$$\frac{d}{dy} \left(\frac{\mu p_c}{\dot{\gamma}} \frac{du_x}{dy} - \frac{\ell^2 \mu \Pi}{\dot{\gamma}} \frac{d^3 u_x}{dy^3} \right) = 0$$

As $p_c = \Pi$,

$$\frac{d}{dy} \left(\frac{\mu \Pi}{\dot{\gamma}} \frac{du_x}{dy} - \frac{\ell^2 \mu \Pi}{\dot{\gamma}} \frac{d^3 u_x}{dy^3} \right) = 0$$

On integrating, we get,

$$\frac{\mu\Pi}{\dot{\gamma}} \frac{du_x}{dy} - \frac{\ell^2 \mu\Pi}{\dot{\gamma}} \frac{d^3 u_x}{dy^3} = S \quad (\text{constant})$$

$$\ell^2 \mu p_c \frac{d^3 u}{dy^3} - (\mu p_c - S) \frac{du}{dy} = 0$$

Let:

$$\lambda^2 = \frac{\mu - \mu_w}{\ell^2 \mu}$$

Here, S is the shear stress at the wall, and from the wall friction boundary condition,

$$\frac{\sigma_{yx}}{\sigma_{yy}} = \mu_w,$$

we have:

$$S = \sigma_{yx} = \mu_w \sigma_{yy} = \mu_w p_c.$$

Then the equation reduces to:

$$\frac{d^3 u}{dy^3} = \lambda^2 \frac{du}{dy}$$

General Solution:

To simplify the algebra and exploit symmetry, we shift the origin to the mid-plane between the plates:

$$\tilde{y} = y - \frac{W}{2}, \quad \tilde{y} \in \left[-\frac{W}{2}, \frac{W}{2} \right]$$

The general solution to the ODE in the shifted coordinate is:

$$u(\tilde{y}) = A \sinh(\lambda \tilde{y}) + B \cosh(\lambda \tilde{y}) + C$$

Boundary Conditions:

- At $\tilde{y} = -\frac{W}{2}$:

$$u\left(-\frac{W}{2}\right) = -u_w + K d_p \left. \frac{du}{d\tilde{y}} \right|_{\tilde{y}=-\frac{W}{2}}$$

- At $\tilde{y} = \frac{W}{2}$:

$$u\left(\frac{W}{2}\right) = u_w + K d_p \left. \frac{du}{d\tilde{y}} \right|_{\tilde{y}=\frac{W}{2}}$$

- At $\tilde{y} = 0$ (symmetry condition):

$$\left. \frac{d^2 u}{d\tilde{y}^2} \right|_{\tilde{y}=0} = 0$$

Solving this boundary value problem yields the analytical solution:

$$\frac{u_x}{u_w} = \frac{1}{2} + \frac{1}{2\beta} \sinh \left[\zeta \left(\frac{W}{2} - y \right) \right]$$

where,

$$\zeta \equiv \left(1 - \frac{\mu_w}{\mu} \right)^{1/2} \frac{1}{\ell}$$

$$\beta \equiv K d_p \zeta \cosh \left(\frac{W\zeta}{2} \right) + \sinh \left(\frac{W\zeta}{2} \right)$$

This solution matches the analytical form reported by Dsouza and Nott [3] for the case of constant volume fraction and zero gravity.

3. Numerical Solution

3.1. Methodology: Finite Difference Method (FDM)

The Finite Difference Method (FDM) is a widely used numerical technique for approximating the solutions of differential equations, especially boundary value problems and partial differential equations, by replacing derivatives with difference quotients on a discrete grid.

3.1.1. Basic Idea of the Finite Difference Method

- **Discretization of the Domain:** The continuous spatial domain is divided into a finite set of grid points.
- **Approximation of Derivatives:** Derivatives in the differential equation are replaced by finite difference formulas involving function values at the grid points.
- **Algebraic System Formation:** The resulting finite difference equations form a system of algebraic equations that can be solved for the unknown values at the grid points.

For example, for a function $u(x)$, the first derivative at a point x_j can be approximated by the forward difference:

$$u'(x_j) \approx \frac{u(x_{j+1}) - u(x_j)}{h}$$

where h is the grid spacing. The second derivative can be approximated by the central difference:

$$u''(x_j) \approx \frac{u(x_{j-1}) - 2u(x_j) + u(x_{j+1}))}{h^2}$$

These approximations convert the differential equation into a set of linear or nonlinear algebraic equations, depending on the original problem.

3.1.2. Method of Undetermined Coefficients for Finite Difference Formulas

To systematically derive finite difference approximations, the method of undetermined coefficients is used:

1. **Stencil Selection:** Choose a set of grid points (the stencil) around the point of interest.
2. **General Linear Combination:** Express the finite difference approximation as a linear combination of function values at these stencil points, with unknown coefficients.
3. **Taylor Expansion:** Expand each function value in a Taylor series about the point of interest.
4. **System Setup:** Set up a system of equations by matching the coefficients of the Taylor expansions to those of the desired derivative.
5. **Solve for Coefficients:** Solve the resulting linear system to find the undetermined coefficients.

Example: Suppose we want a finite difference approximation for $u'(x_j)$ using points x_j , x_{j+1} , and x_{j-1} . Assume:

$$u'(x_j) \approx a u(x_{j-1}) + b u(x_j) + c u(x_{j+1})$$

Expanding $u(x_{j+1})$ and $u(x_{j-1})$ in Taylor series about x_j , and matching the coefficients of $u'(x_j)$, $u(x_j)$, $u''(x_j)$, etc., leads to a system of equations for a , b , and c . Solving this system yields the coefficients for the finite difference formula.

Summary Table: Steps in the Method of Undetermined Coefficients

Step	Description
Choose stencil	Select grid points to use in the approximation
Write general formula	Express as a linear combination with unknown coefficients
Expand in Taylor series	Expand each function value about the point of interest
Match terms	Equate coefficients of like powers to those in the target derivative
Solve for coefficients	Solve the resulting linear system

Table 1: Steps in deriving finite difference formulas using the method of undetermined coefficients.

References

Randall J. LeVeque, *Finite Difference Methods for Ordinary and Partial Differential Equations: Steady-State and Time-Dependent Problems*, SIAM, 2007[4] .

3.2. Model Predictions for simple shear

3.2.1. Governing Equations

For steady, fully developed flow, the relevant momentum balances to be satisfied are:

$$\frac{d\sigma_{yy}}{dy} = 0, \quad \frac{d\sigma_{yx}}{dy} = 0 \quad (3.1)$$

Substituting the constitutive relation for the stress (Equation 1.1a,b,c) into the above balances, we obtain the equations that govern $u_x(y)$ and $\phi(y)$.

$$\frac{d}{dy} \left(\frac{\mu P_c}{\dot{\gamma}} \frac{du_x}{dy} - \frac{\ell^2 \mu \Pi}{\dot{\gamma}} \frac{d^3 u_x}{dy^3} \right) = 0, \quad \frac{dP_c}{dy} = 0 \quad (3.2)$$

3.2.2. Boundary Conditions

- At the **top wall** (moving with velocity u_w), as described in Figure 1

$$u_x - u_w = n_y K d_p \frac{du_x}{dy}, \quad \frac{\sigma_{yx}}{\sigma_{yy}} = \mu_w$$

- At the **bottom wall**:

$$u_x - 0 = K d_p \frac{du_x}{dy}$$

- At the **mid-plane** ($y = W/2$):

$$\frac{d^2 u_x}{dy^2} = 0$$

Here, u_w is the wall velocity, n_y is the y-component of the unit normal at the wall pointing into the granular medium, K is the slip coefficient, d_p is the mean particle diameter, and μ_w is the wall friction coefficient.

The above conditions apply only when the material adjacent to the wall is undergoing plastic deformation.

3.2.3. Numerical Implementation

To analyse the coupling between volume fraction and velocity in the gravity-free plane shear configuration, numerical solutions were obtained for the case $d_p = d_w$, following the framework

of Dsouza and Nott [3]. The governing equations were first non-dimensionalized using appropriate scaling factors for length and stress, which simplified the numerical implementation and ensured the generality of the solution.

The finite difference method was employed, using a second-order central difference scheme for interior points and second-order forward/backward schemes at the boundaries. The implementation of derivative coefficients was handled using a helper function, `fdcoeff.m`, which was included as part of the numerical codebase and is appended to this report for reference. The resulting nonlinear algebraic equations for u_x and ϕ at the N discretized values of y were solved using the nonlinear equation solver `fsolve` in MATLAB.

The volume fraction profile was solved first and used in the momentum equation. A constant of integration was determined via a shooting method to satisfy the average volume fraction condition $\bar{\phi} = 0.584$. With the volume fraction known, the velocity profile was computed using the same numerical approach.

To ensure the accuracy of the numerical solution, the results are quantitatively validated by comparing them with data extracted from the original numerical results reported in Dsouza and Nott [3]. The close agreement between the two datasets confirms the correctness and stability of the implemented method.

The MATLAB code files used to implement the numerical scheme and obtain the volume fraction and velocity profiles are provided below for reference.

3.2.4. Results and Discussion

Figure 2 shows the velocity and volume fraction profiles in plane shear flow in the absence of gravity, compared with DEM simulations for the same configuration. The model predictions are obtained by solving Equation (3.1) with boundary conditions given by Equations (3.2) at both walls and Equations (3.4a), (3.4c), and (3.4d).

The agreement between the model predictions and the DEM simulations is remarkably good, although this is not the primary focus of discussion here. Rather, the model predictions emphasize the strong coupling between the velocity and volume fraction fields—a greater variation in ϕ leads to a sharper variation in velocity (and consequently the shear rate).

The resulting profile of the volume fraction exhibits mild spatial variation and is coupled with the velocity field, consistent with experimental observations and predictions from the non-local constitutive model. As expected for the gravity-free plane shear configuration, the velocity profile is found to be antisymmetric about the mid-plane, while the volume fraction profile is symmetric.

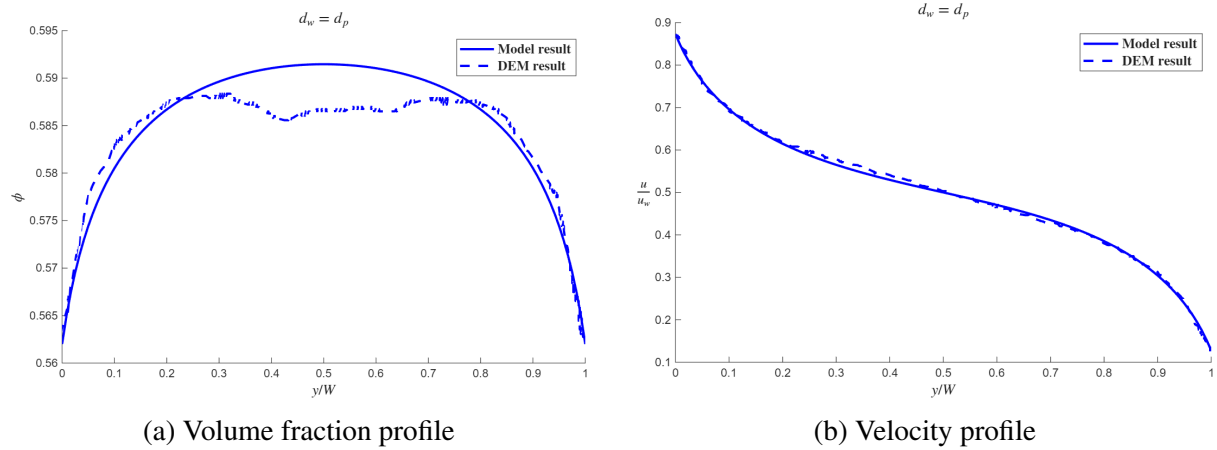


Figure 2: Profiles of the volume fraction (a) and velocity (b) for plane shear in the absence of gravity, for a Couette gap $W = 40d_p$ and mean volume fraction $\bar{\phi} = 0.585$. The dashed lines are results from DEM simulations using wall particles of two sizes (see Figure 1). The solid lines represent model predictions with $K = 1.65$ and $\mu_w = 0.33$ (fitted for $d_w = d_p$).

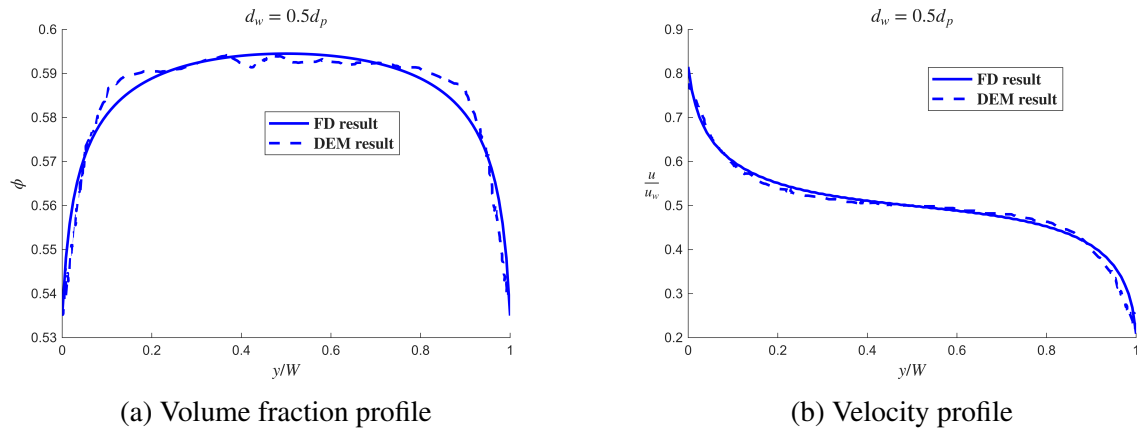


Figure 3: Profiles of the volume fraction (a) and velocity (b) for plane shear in the absence of gravity, for a Couette gap $W = 40d_p$ and mean volume fraction $\bar{\phi} = 0.585$. The dashed lines are results from DEM simulations using wall particles of two sizes (see Figure 1). The solid lines represent model predictions with $K = 0.95$ and $\mu_w = 0.1$ (fitted for $d_w = 0.5d_p$).

Obtained Plots

Other Non-local Models – $\phi(I)$ rheology

$$\phi = \phi_0 - \frac{A \dot{\gamma}}{\sqrt{P}}$$

$$P = \frac{A^2 \dot{\gamma}^2}{(\phi_0 - \phi)^2}$$

where P = pressure

Here, the value of ϕ_0 is taken as ϕ_{\max} , as the pressure is observed to diverge at the jamming fraction (maximum solid fraction).

- This equation is also known to capture dilatancy, but in the slow flow regime, the inertia of the system is not significant, and in this relation, the pressure is scaled by an inertial term, i.e., shear rate, which predicts inconsistent results at the boundaries of the spatial domain.
- This can be better understood by looking at the comparison in the next slide.

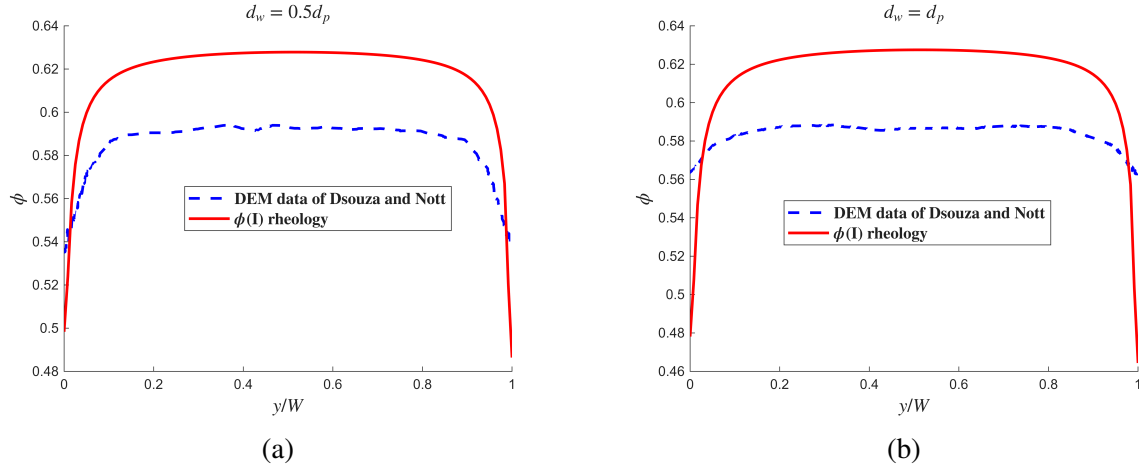


Figure 4: Comparison of obtained profiles with DEM results and $\phi(I)$ rheology. The parameter $\frac{A}{\sqrt{P}}$ was optimized as 0.0202 for (a) and 0.0233 for (b).

3.3. Model Predictions for Couette flow

3.3.1. Governing Equations

The governing equations are the balances of mass, and the r and θ components of momentum. For steady axisymmetric flow, the mass balance is trivially satisfied, and the r and θ momentum balances reduce to:

$$\frac{\partial \sigma_{rr}}{\partial r} = 0, \quad \frac{1}{r^2} \frac{\partial}{\partial r} \left(r^2 \sigma_{r\theta} \right) = 0$$

On substituting the constitutive relation for σ (Eq. 3.1), the momentum balances (Eq. 3.2) take the form:

$$\frac{d}{dr} \left[\Pi - l^2 \frac{d\Pi}{d\phi} \left(\frac{d^2\phi}{dr^2} + \frac{1}{r} \frac{d\phi}{dr} \right) \right] = 0 \quad (3.3)$$

$$\frac{1}{r^2} \frac{d}{dr} \left[r^2 \frac{\mu P_c}{\dot{\gamma}} \left(\frac{du_\theta}{dr} - \frac{u_\theta}{r} \right) - r^2 l^2 \frac{\mu \Pi}{\dot{\gamma}} \left(\frac{d^3 u_\theta}{dr^3} + \frac{1}{r^2} \frac{du_\theta}{dr} - \frac{u_\theta}{r^3} \right) \right] = 0 \quad (3.4)$$

where

$$\dot{\gamma} = \left| \frac{du_\theta}{dr} - \frac{u_\theta}{r} \right| \quad (3.5)$$

3.3.2. Boundary Conditions

To close Eq. (3.3), Eq. (3.4), four boundary conditions for u_θ and three for ϕ are required. Unlike fluids, granular media usually slip at rigid boundaries, and accounting for slip is often important. Using this condition and the wall friction boundary condition, we have

$$u_\theta - u_w = K_{dp} \left(\frac{du_\theta}{dr} + \frac{u_\theta}{r} \right), \quad -\frac{\sigma_{r\theta}}{\sigma_{rr}} = \mu_w \quad \text{at } r = r_i$$

$$u_\theta = 0, \quad \frac{du_\theta}{dr} = 0 \quad \text{at } r = r_o$$

where μ_w is the friction coefficient between the inner wall and the granular material. At steady state, the shear stress $\sigma_{r\theta}$ decreases with r , while the normal stress σ_{rr} is constant, whence $\left| \frac{\sigma_{r\theta}}{\sigma_{rr}} \right|$ decreases with r .

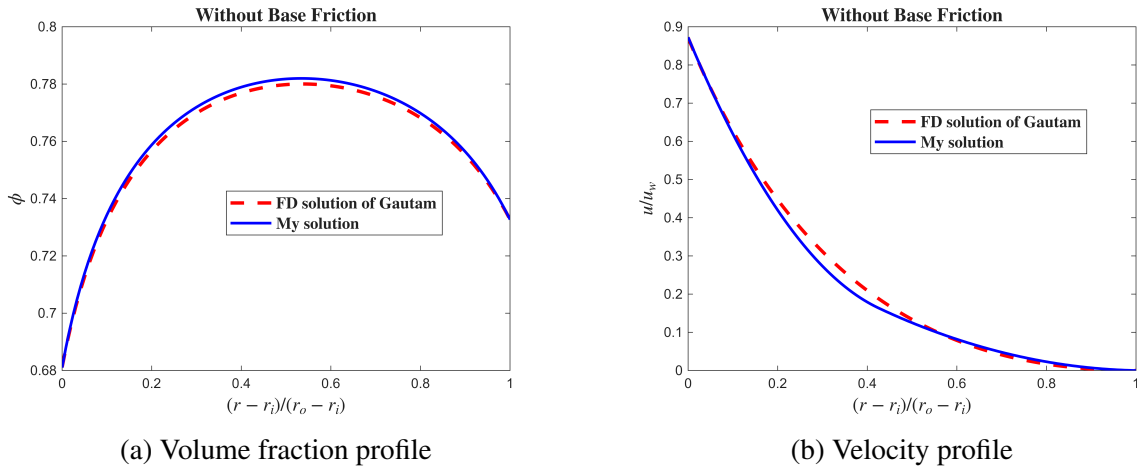


Figure 5: Experimental data and model predictions for the outer cylinder with LB, see Figure 1. (a) Data for the area fraction $\phi(r)$ before shear is commenced and at steady state, compared with the model prediction using the best-fit parameter values: $n_1 = 2$, $n_2 = 1$, and $\alpha = 30$ Pa. (b) Data for the velocity $u_\theta(r)$ at steady state, compared with the model predictions using the best-fit parameter values: $\mu_w/\mu = 0.99$, $\mu_{\text{base}}/\mu = 3.76$, and $K = 0.63$.

Note: The current results are not fully consistent with the experimental trends. Code debugging is in progress, and further validation is ongoing.

Future Work

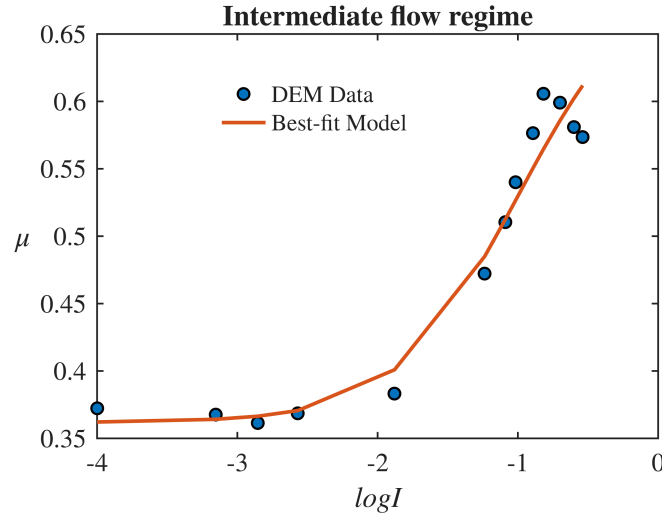


Figure 6: DEM Data and Best-fit Model for the intermediate flow regime.

Data for the above plot was collected from the DEM results (Cylindrical Couette flow) of Gautam Bhaiya.

$$\mu(I) = \mu_s + \frac{\mu_2 - \mu_s}{\frac{I_0}{I} + 1}$$

Values of the parameters obtained for best fit:

$$\mu_2 - \mu_s = 0.3367$$

$$I_0 = 0.1005$$

$$\mu_s = 0.3618$$

- Extend the Dsouza–Nott model to the intermediate inertial regime in order to better understand and interpret the model behavior in these flow regimes. Like the equation below, can now be written in the form where,

$$\frac{1}{r^2} \frac{d}{dr} \left[r^2 \frac{\mu(I) P_c}{\dot{\gamma}} \left(\frac{du_0}{dr} - \frac{u_0}{r} \right) \right] - r^2 \frac{\mu(I) I}{\dot{\gamma}} \left(\frac{d^3 u_0}{dr^3} + \frac{1}{r^2} \frac{du_0}{dr} - \frac{u_0}{r^3} \right) = 0$$

4. MATLAB Implementation

4.1. Finite Difference Coefficient Determination

The following MATLAB function computes the coefficients for finite difference approximations of derivatives of arbitrary order at a specified location, based on the method described by B. Fornberg (SIAM Review 40, 1998). This function is robust for both uniform and non-uniform grids.

```
function c = fdcoeffV(k,xbar,x)
% Compute coefficients for finite difference approximation for the
% derivative of order k at xbar based on grid values at points in x.
%
% This function returns a row vector c of dimension 1 by n, where n=
%   length(x),
% containing coefficients to approximate  $u^{\{k\}}(xbar)$ ,
% the k'th derivative of u evaluated at xbar, based on n values
% of u at x(1), x(2), ... x(n).
%
% If U is a column vector containing u(x) at these n points, then
% c*U will give the approximation to  $u^{\{k\}}(xbar)$ .
%
% Note for k=0 this can be used to evaluate the interpolating
%   polynomial
% itself.
%
% Requires length(x) > k.
% Usually the elements x(i) are monotonically increasing
% and x(1) <= xbar <= x(n), but neither condition is required.
% The x values need not be equally spaced but must be distinct.
%
% This program should give the same results as fdcoeffV.m, but for
%   large
% values of n is much more stable numerically.
%
% Based on the program "weights" in
%   B. Fornberg, "Calculation of weights in finite difference
%   formulas",
%   SIAM Review 40 (1998), pp. 685-691.
%
% Note: Forberg's algorithm can be used to simultaneously compute
%   the
```

```

% coefficients for derivatives of order 0, 1, ..., m where m <= n-1.
% This gives a coefficient matrix C(1:n,1:m) whose k'th column gives
% the coefficients for the k'th derivative.
%
% In this version we set m=k and only compute the coefficients for
% derivatives of order up to order k, and then return only the k'th
% column
% of the resulting C matrix (converted to a row vector).
% This routine is then compatible with fdcoeffV.
% It can be easily modified to return the whole array if desired.
%
% From http://www.amath.washington.edu/~rjl/fdmbook/ (2007)

n = length(x);
if k >= n
    error('***_length(x)_must_be_larger_than_k')
end

m = k; % change to m=n-1 if you want to compute coefficients for
all
% possible derivatives. Then modify to output all of C.
c1 = 1;
c4 = x(1) - xbar;
C = zeros(n-1,m+1);
C(1,1) = 1;
for i=1:n-1
    i1 = i+1;
    mn = min(i,m);
    c2 = 1;
    c5 = c4;
    c4 = x(i1) - xbar;
    for j=0:i-1
        j1 = j+1;
        c3 = x(i1) - x(j1);
        c2 = c2*c3;
        if j==i-1
            for s=mn:-1:1
                s1 = s+1;
                C(i1,s1) = c1*(s*C(i1-1,s1-1) - c5*C(i1-1,s1))/c2;
            end
            C(i1,1) = -c1*c5*C(i1-1,1)/c2;
        end
    end
end

```

```
    end
    for s=mn:-1:1
        s1 = s+1;
        C(j1,s1) = (c4*C(j1,s1) - s*C(j1,s1-1))/c3;
    end
    C(j1,1) = c4*C(j1,1)/c3;
    end
    c1 = c2;
    end

c = C(:,end)';
% last column of c gives desired row vector
end
```

Listing 1: Finite Difference Coefficient Generator (fdcoeffV.m)

5. Conclusion

- Understood the **non-local constitutive model** for granular flows (Dsouza and Nott).
- Learned to formulate **momentum balances in cylindrical coordinates**.
- Applied the **Finite Difference Method (FDM)** for solving **steady-state problems** (ODEs).
- Learned the method of undetermined coefficients for finite difference schemes.
- Developed skills in parameter fitting, model validation, and comparison with DEM data.
- Enhanced **MATLAB programming skills** for simulation and visualization.
- Developed a clear understanding of how to **numerically approach a problem**—from writing governing equations and non-dimensionalization, to solving, fitting, and interpreting results.

6. Acknowledgement

I would like to express my sincere gratitude to the **Indian Academy of Sciences** for providing me the opportunity to participate in the prestigious **Summer Research Fellowship (SRF)** Program. This platform has played a crucial role in broadening my academic and research horizons.

I would like to extend my deepest thanks to **Professor Prabhu R Nott, Department of Chemical Engineering, IISc Bangalore**, for his invaluable mentorship and continuous support during the course of my project titled “Modelling of Slow Granular Flow.”

I am also sincerely grateful to **Gautam** bhaiya for his support, encouragement, and helpful insights throughout the internship. His guidance played an important role in shaping my experience and progress during this project.

I also wish to sincerely thank all the **lab members** for their warm welcome, constant encouragement, and assistance throughout the internship. Their collaborative spirit and willingness to share knowledge made this experience even more fulfilling.

I am truly grateful for the opportunity to be part of such a distinguished research community.

References

- [1] GDR MiDi gdrmidi@polytech.univ-mrs.fr <http://www.lmgc.univ-montp2.fr/MIDI/>. On dense granular flows. *The European Physical Journal E*, 14:341–365, 2004.
- [2] Pierre Jop, Yoël Forterre, and Olivier Pouliquen. A constitutive law for dense granular flows. *Nature*, 441(7094):727–730, 2006.
- [3] Peter Varun Dsouza and Prabhu R Nott. A non-local constitutive model for slow granular flow that incorporates dilatancy. *Journal of Fluid Mechanics*, 888:R3, 2020.
- [4] Randall J LeVeque. *Finite difference methods for ordinary and partial differential equations: steady-state and time-dependent problems*. SIAM, 2007.